applied sciences

MDPI

Communication

Design and Functionality of a Prototype for Cold Needle Perforation of Wheat

Luca Stäheli, Lisa Schwab, Mathias Kinner and Nadina Müller *

Department for Life Sciences und Facility Management, Institute for Food and Beverage Innovation (ILGI), Research Group for Food Technology, Zürcher Hochschule für Angewandte Wissenschaften (ZHAW), 8820 Wädenswil, Switzerland; sthi@zhaw.ch (L.S.); kinr@zhaw.ch (M.K.)
* Correspondence: nadina.mueller@zhaw.ch

Abstract: Wheat is a vital crop in global food security, but up to 25% of the wheat harvested is contaminated with mycotoxins that have detrimental effects on human health. To address this issue, biological detoxification strategies have been developed using microorganisms and enzymes. Perforating the whole wheat kernel using cold needle perforation (CNP) followed by a detoxification step could be a promising approach to reduce cross-contamination during the milling of mycotoxin-containing wheat. In this study, a pilot-scale CNP prototype was developed to perforate wheat kernels, and its effectiveness was evaluated. The height-adjustable perforation unit consists of 3120 needles. The throughput of the CNP prototype was adjusted to 6 kg/h, and the kernels were perforated for 1, 5, or 10 cycles. The results show that the CNP prototype effectively perforates wheat kernels, as evidenced by the significant increase in pore count. Fluorescence microscopy confirmed the penetration of particles in the size range of enzymes and microorganisms into the kernel. This study demonstrates the successful scale-up of CNP for wheat kernel perforation and highlights the potential of CNP as a cost-effective and efficient method for the biological detoxification of mycotoxin-contaminated wheat.

Keywords: prototype; upscaling; cold needle perforation; treatment; wheat; mycotoxin

Citation: Stäheli, L.; Schwab, L.; Kinner, M.; Müller, N. Design and Functionality of a Prototype for Cold Needle Perforation of Wheat. *Appl. Sci.* **2023**, *13*, 6266. https://doi.org/10.3390/app13106266

Academic Editor: Antonio Valero

Received: 21 April 2023
Revised: 16 May 2023
Accepted: 17 May 2023
Published: 20 May 2023

1. Introduction

Wheat is one of the most important cereal crops for human nutrition [1,2] and makes up approximately 20% of the total global calorie intake [3]. According to the Food and Agriculture Organization (FAO), 750 million tonnes are harvested globally and 25% of the harvested wheat is affected by moulds and mycotoxins [4,5]. Mycotoxins are secondary metabolites of moulds and have an adverse effect on human health, also referred to as mycotoxicosis [6]. Possible health effects range from acute gastrointestinal issues to the development of cancer. Intoxication with mycotoxins can occur through renal absorption or through the inhalation of spores [7]. Thus, mycotoxins form a substantial public health concern.

The toxins are unevenly distributed in the wheat kernel, with the highest concentration present in the bran layer. Thus, a cost-effective method of reducing the toxic load and conforming with legal limits is to physically separate the endosperm from the bran layers. This results, however, in a loss of up to 20% of total mass and at the same time reduces the dietary fibre content, micronutrient and mineral content, and other valuable components [8].

Recently, biological detoxification strategies have been developed in wheat kernels using functional microorganisms and enzymes [9,10]. To reduce cross contamination during the milling of mycotoxin-containing wheat, the detoxification of whole wheat kernels is a promising approach.

To achieve this, the hydrophobic aleurone layer must be disrupted first to enable the diffusion of active substances throughout the layers. This disruption has been shown to be best achieved through cold needle perforation (CNP), as previously shown by Stäheli et al. [11].

The authors further demonstrated that fluorescent particles in the size range of enzymes (5 nm) and microorganisms (10 µm) were able to pass into the kernel through fluorescence image analysis. This work reports on the scale-up of cold needle perforation for wheat kernel perforation and the effectiveness of the resulting CNP prototype.

2. Materials and Methods

2.1. Wheat Kernels

All trials were conducted using wheat samples in two different quality classes according to Swiss standards: quality class TOP (Swissmill AG, 10580 B, Zurich, Switzerland), representing the highest quality class, and Wheat I (Swissmill AG, 10581 C, Zurich, Switzerland), with water contents of 12.57% (*w*/*w*) and 12.44% (*w*/*w*), respectively. Wheat classes in Switzerland are defined by Agroscope and Swissgranum taking a broad range of laboratory analyses as well as standardized baking trials into account. TOP and Wheat I need to have a wet gluten content of more than 31% and at least 29%, respectively, and represent two of the most common qualities used to produce wheat bread.

2.2. Cold Needle Perforation Pilot-Scale Prototype

A cold needle perforation (CNP) prototype was built in-house. The wheat kernel application is done automatically to increase dosage reproducibility and distribute the wheat kernels on the conveyor belt. It consists of a hopper (Retsch GmbH, DR100, Haan, Germany) and a 270 mm long 3D-printed chute (Extrudr I FD3D, GreenTEC, Lauterach, Austria). The conveyor belt is made from food-grade thermoplastic polyurethane (Habasit GmbH, FMW-3EZWH-P1, Eppertshausen, Germany), cushioned by a polytetrafluoroethylene-covered sponge (Hans Werner GmbH, product number 129.33 (280 mm × 140 mm × 20 mm), Laupheim, Germany), is powered by a worm-geared motor (Vector Aandrijftechniek B.V., V380-415Y, Rotterdam, The Netherlands) and its speed is controlled by a single-phase frequency converter (ABB Ltd., ACS 141-K37-1, Zurich, Switzerland). The perforation in the CNP prototype is achieved by a roll of 3′120 1.8 mm long needles consisting of 65 circular saw blades (Bosch GmbH, Dremel saw blade 546, Farmington Hills, MI, USA) separated by 1 mm thick 3D-printed polylactic acid (PLA) discs (Redline Filament GmbH, PLA filament RAL 7011, Neuss, Germany). To avoid breakage of the perforation unit, a saw tooth geometry with increased stability was chosen. This perforation unit is attached to a speed- and height-adjustable axis. Through the height adjustment via a fine pitch spindle and two guiding bolts, the gap size is set to either −1 mm or 0 mm, thus creating different pressure levels on the kernels during perforation. Different shear forces can be imposed on the kernels through the speed adjustment via an adjustable voltage source (BaSeTech Batterie Service GmbH, BT-3010, Hamburg, Germany) of the motor (EPH Elektronik GmbH, DO11190393B00/3019, Besingheim-Ottmarskeim, Germany). The conveyor belt and feeder speed were adjusted to a throughput of 6 kg/h, and the kernels where perforated for 1, 5, or 10 cycles. A schematic drawing and an image of the CNP prototype are shown in Figure 1.

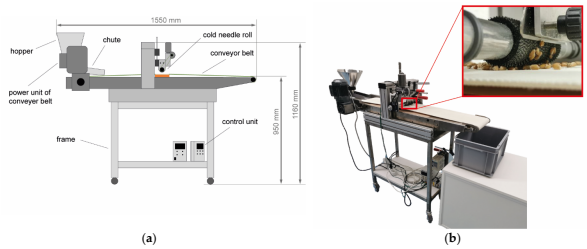

Figure 1. Schematic drawing (**a**) and image (**b**) of the cold needle perforation (CNP) prototype, including a close-up view of the perforation unit (red).

2.3. Determination of Pore Count

In order to quantify perforation success, a randomized sampling of 10 kernels was conducted and pores were measured using a digital microscope (Tagarno, FHD Trend, Horsens, Denmark) with 10 times optical zoom and 40 times digital zoom. The aperture was set to f/4.0 with an exposure time of 1/25 s. The pores on each kernel were counted from front to left side according to Figure 2.

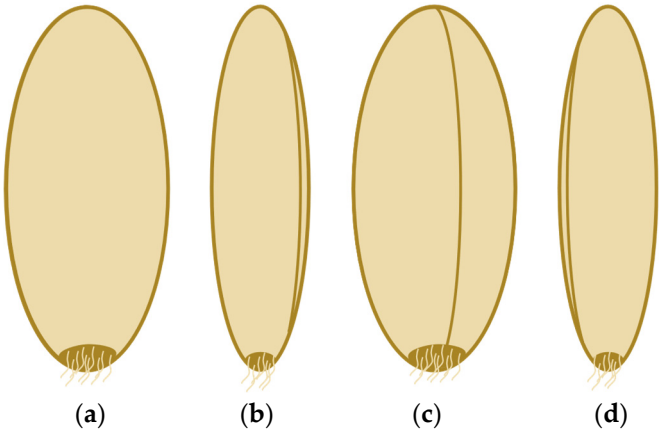

Figure 2. Schematic drawing of wheat kernel for side definition: (**a**) front, (**b**) right side, (**c**) germ-scar side, and (**d**) left side.

2.4. Fluorescence Microscopy

The wheat kernels were assessed according to the protocol described by Stäheli et al. [11] using a fluorescence microscope (ECHO, Revolve, San Diego, CA, USA) with the filter sets DAPI (excitation (EX): 385/30, emission (EM): 450/50, dichromatic mirror (DM): 425), FITC (EX: 470/40, EM: 525/50, DM: 495), and TRITC (EX: 530/40, EM: 590/50, DM: 560).

2.5. Scanning Electron Microscopy (SEM)

The sputtering and visual assessment was done according to the method previously described by Stäheli et al. [11]. The wheat kernels were sputtered with gold for 30 s with 20 mA (Quorum Technologies Ltd., Q150RS, Laughton, UK) to decrease the interference of humidity and the flow of electrons before being visually analysed using a scanning electron microscope (FEI Company, Quanta FEG250, Hillsboro, OR, USA). The detection of pores was conducted under micro-vacuum conditions with an acceleration voltage of 10 kV, and the detection spot size was set to 3.0. The size of each formed pore was measured with the default software (FEI Company, xT microscope Control Software Version 6.2.8.3161, Hillsboro, OR, USA).

2.6. Determination of Broken Grains

A vibratory sieve shaker (Retsch GmbH, AS 200 Control, Haan, Germany) was used before and after the perforation treatment to separate the broken grains form the intact fraction. First, 50 g of kernels were weighed and applied to a sieve stack with mesh size of 2.8 mm, 2 mm, 1 mm, and a bottom plate, and the total sieving time was set to 2 min. After sieving, each fraction was weighed again and the kernels passing through the sieve with a mesh size of 2 mm were classified as the broken fraction (%). The analysis was done in triplicate for each quality class and perforation cycle.

2.7. Statistical Analysis

Analysis of variance ($\alpha = 0.05$) was conducted and means were separated according to Fisher's least significant difference procedure ($p < 0.05$) using R (R Foundation for Statistical Computing, R4.2.1, Vienna (AUS)) and RStudio (RStudio PBC, Boston, MA, USA). Statistical

significance ($p < 0.05$) was determined, and significant differences were indicated by using separate-letter reporting.

3. Results and Discussion

3.1. Effect of Gap Size on Perforation Results and Broken Grain Content

The gap size adjustment to both −1 mm or 0 mm had no significant effect on the perforation counts in the TOP wheat kernel surfaces (Figure 3), as with −1 mm and 0 mm a mean pore count of 7.9 and 7.1 was achieved, respectively. However, it can be concluded that the rate of breakage is dependent on the gap size, as a reduced gap size and thus increased pressure during perforation results in significantly more breakage, with 9.2% and 4.3% for a gap size of −1 mm and 0 mm, respectively.

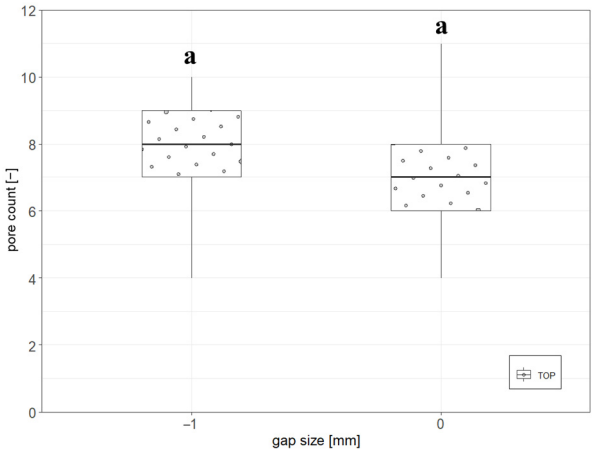

Figure 3. Pore formation depending on gap size of −1 mm or 0 mm after five perforation cycles ($n = 30$) of TOP wheat kernels. Different letters indicate significant differences ($p < 0.05$).

The visual assessment of the wheat kernels showed (Figure 4) that the hyaline layer (grey-purple coloured) and aleurone layer (blue) had been perforated irrespective of the gap size of the cold needle perforation used. In summary, the results indicated that a smaller gap size of 0 mm results in significantly reduced production loss while maintaining a sufficient penetration depth.

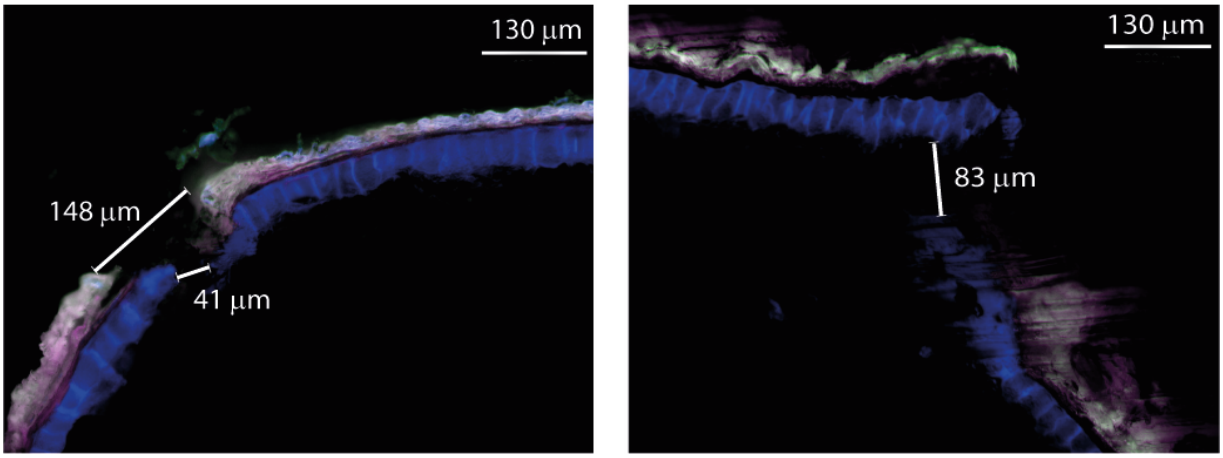

(**a**) (**b**)

Figure 4. TOP wheat grains after cold needle perforation treated at a gap width of 0 mm (**a**) and −1 mm (**b**). Overlay of the channels DAPI, FITC, and TRITC. The aleurone layer is visible in blue; the hyaline layer is visible in grey-purple.

3.2. Effect of Perforation Cycles and Wheat Grain Quality on Pore Formation

While the applied pressure played an insignificant role in the perforation count, the number of perforation cycles showed a linear increase in the number of pores formed (Figure 5), but no significant differences could be observed between TOP and Wheat I qualities. This linear dependency of the perforation count on the perforation cycle indicates that the wheat kernels pass under the needle wheel in every cycle which is consistent with what was observed during the trials.

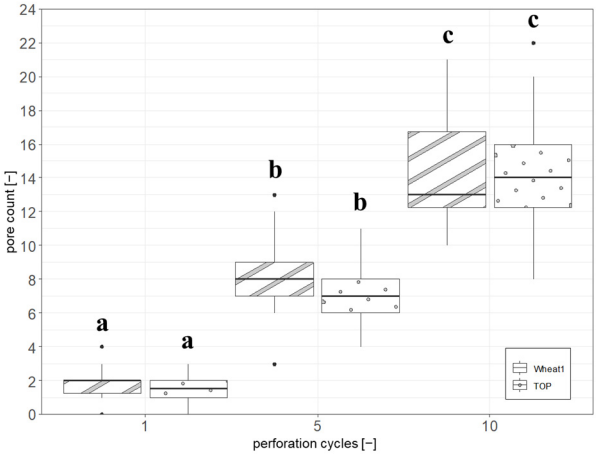

Figure 5. Pore formation after 1, 5, or 10 perforation cycles with a gap size of 0 mm and depending on wheat grain quality (n = 30). Different letters indicate significant differences ($p < 0.05$).

The same linear increase could be observed with the breakage of the kernels with <1%, 4–5%, and 9–10% for 1, 5, and 10 cycles, respectively. No significant effect of wheat grain quality on the breakage could be detected.

Figure 6 shows a typical elongated incision achieved with the pilot-scale CNP device. The length of the incision shrinks with the increasing depth of the penetration due to the tooth-like needle geometry.

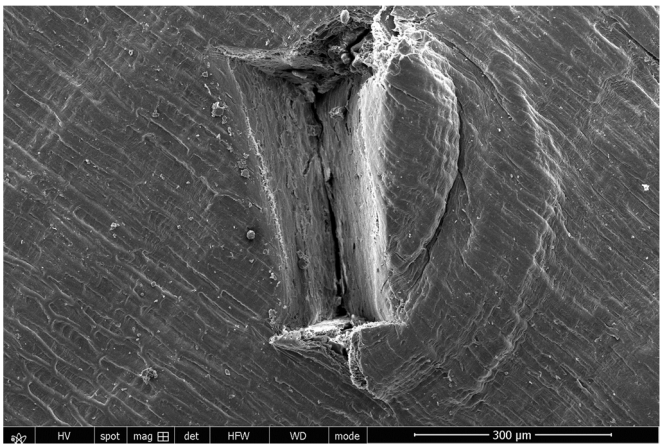

Figure 6. Wheat kernel (TOP quality) perforated with cold needle perforation at a gap size of 0 mm. REM images taken with an accelerating voltage of 10 kV at 207× magnification.

3.3. Effect of Kernel Orientation on Pore Count

Pore formation on the kernels was unevenly distributed across the surface of each kernel (Figure 7). Significantly more pores were produced on the front (opposite to germ scar) compared to left side. This uneven distribution is probably influenced by several factors, such as the uneven distribution of mass relative to the axis of rotation (inertia)

which initially leads to the kernel landing on the curved front side (Figure 8a) when falling from the chute, followed by the rotation to either side (Figure 8b) [12]. As the front of the wheat kernel and both sides have a curved surface, the kernel is more likely to stop on the germ-scar side, which has a plateau-like form rather than a curved form, thus resulting in the perforation of the front side (Figure 8c). However, the difference between the pore count of the right and left side is most probably systemic, as the pores on the kernel were assessed from front to left (Figure 2) and thus the pores on the left side may have already been associated with the front or germ-scar side as the borders, which would result in a reduced pore count on the left side of the wheat kernel.

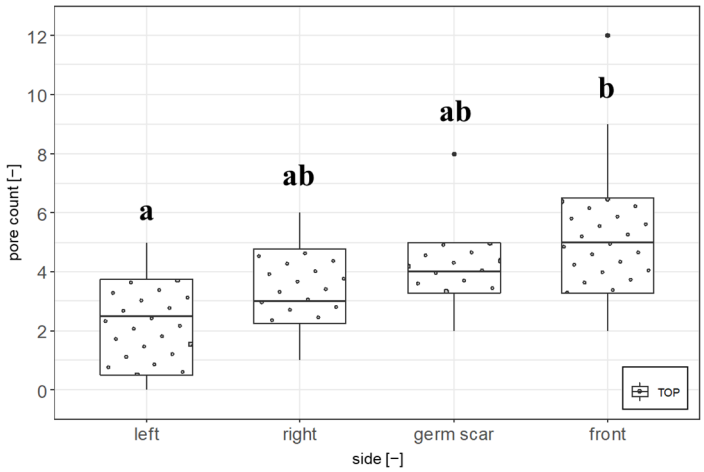

Figure 7. Perforation count depending on kernel side after 10 perforation cycles (n = 10) of TOP wheat kernels. Different letters indicate significant differences ($p < 0.05$).

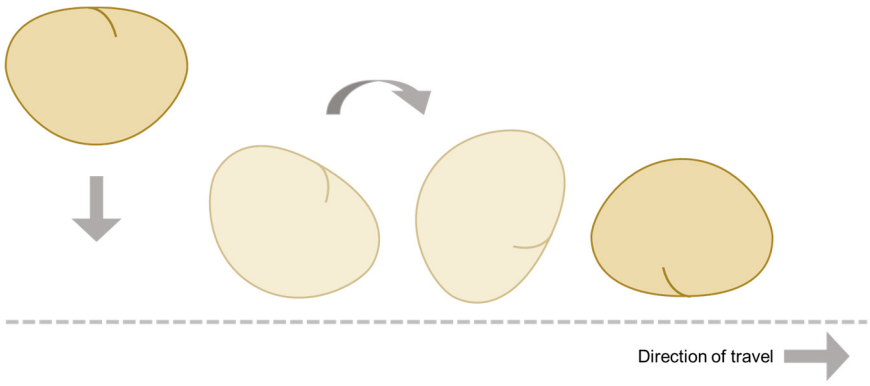

Figure 8. Explanation for uneven pore formation. Wheat kernel landing on (**a**) the front side, followed by (**b**) a rotation to either side due to the curved surface and (**c**) landing on the germ-scar side, resulting in the perforation of the front side.

4. Conclusions

The CNP prototype showed that it is possible to upscale cold needle perforation for wheat kernels to a continuous process with a throughput of up to 6 gg per hour. Between 93.3% (TOP) and 99% (Wheat I) of the wheat kernels featured 10 or more formed pores after 10 cycles, thus showing a consistent and repeatable treatment of the kernels. As a next step, the effectiveness of the perforations to allow active substances to pass the bran layers needs to be established in application trials.

Author Contributions: L.S. (Luca Stäheli): project administration, writing; L.S. (Lisa Schwab): investigation, validation; M.K.: data curation; N.M.: funding acquisition, supervision. All authors have read and agreed to the published version of the manuscript.

Funding: This research was partly funded by the Health Research Hub at Zurich University of Applied Sciences.

Institutional Review Board Statement: Not applicable.

Informed Consent Statement: Not applicable.

Data Availability Statement: The data presented in this study are available on request from the corresponding author. The data are not publicly available due to privacy.

Acknowledgments: We would like to thank Pius Meier for contributing with his expertise in prototyping and assembling the CNP prototype. We would also like to thank John Bennett for proofreading this paper.

Conflicts of Interest: The authors declare no conflict of interest.

References

1. Peña, R.J. Current and Future Trends of Wheat Quality Needs. In *Wheat Production in Stressed Environments*; Buck, H.T., Nisi, J.E., Salomón, N., Eds.; Springer: Dordrecht, The Netherlands, 2007; pp. 411–424. [CrossRef]
2. Gupta, P.K.; Mir, R.R.; Mohan, A.; Kumar, J. Wheat Genomics: Present Status and Future Prospects. *Int. J. Plant Genom.* **2008**, *2008*, e896451. [CrossRef] [PubMed]
3. Brenchley, R.; Spannagl, M.; Pfeifer, M.; Barker, G.L.A.; D'Amore, R.; Allen, A.M.; McKenzie, N.; Kramer, M.; Kerhornou, A.; Bolser, D.; et al. Analysis of the bread wheat genome using whole-genome shotgun sequencing. *Nature* **2012**, *491*, 705–710. [CrossRef] [PubMed]
4. Eskola, M.; Kos, G.; Elliott, C.T.; Hajšlová, J.; Mayar, S.; Krska, R. Worldwide contamination of food-crops with mycotoxins: Validity of the widely cited "FAO estimate" of 25. *Crit. Rev. Food Sci. Nutr.* **2020**, *60*, 2773–2789. [CrossRef] [PubMed]
5. Pereira, V.L.; Fernandes, J.O.; Cunha, S.C. Mycotoxins in cereals and related foodstuffs: A review on occurrence and recent methods of analysis. *Trends Food Sci. Technol.* **2014**, *36*, 96–136. [CrossRef]
6. Peraica, M.; Radić, B.; Lucić, A.; Pavlović, M. Toxic effects of mycotoxins in humans. *Bull. World Health Organ.* **1999**, *77*, 754–766. [PubMed]
7. Fung, F.; Clark, R.F. Health Effects of Mycotoxins: A Toxicological Overview. *J. Toxicol. Clin. Toxicol.* **2004**, *42*, 217–234. [CrossRef] [PubMed]
8. Laca, A.; Mousia, Z.; Díaz, M.; Webb, C.; Pandiella, S.S. Distribution of microbial contamination within cereal grains. *J. Food Eng.* **2006**, *72*, 332–338. [CrossRef]
9. Shcherbakova, L.; Rozhkova, A.; Osipov, D.; Zorov, I.; Mikityuk, O.; Statsyuk, N.; Sinitsyna, O.; Dzhavakhiya, V.; Sinitsyn, A. Effective Zearalenone Degradation in Model Solutions and Infected Wheat Grain Using a Novel Heterologous Lactonohydrolase Secreted by Recombinant Penicillium canescens. *Toxins* **2020**, *12*, 475. [CrossRef] [PubMed]
10. Zhu, Y.; Hassan, Y.I.; Lepp, D.; Shao, S.; Zhou, T. Strategies and Methodologies for Developing Microbial Detoxification Systems to Mitigate Mycotoxins. *Toxins* **2017**, *9*, 130. [CrossRef] [PubMed]
11. Stäheli, L.; Kinner, M.; Müller, N. Effectiveness of perforation methods for wheat kernels. *Cereal Technol.* **2022**, *2022*, 4–15.
12. Newton, I.; Chittenden, N.W. *Newton's Principia: The Mathematical Principles of Natural Philosophy*; G. P. Putnam's Sons: New York, NY, USA, 1850.